Experimental Detection of Quantum Channels

Adeline Orieux,[1,*] Linda Sansoni,[1] Mauro Persechino,[1] Paolo Mataloni,[1,2] Matteo Rossi,[3] and Chiara Macchiavello[3]

[1]*Dipartimento di Fisica, Sapienza Università di Roma, Piazzale Aldo Moro, 5, I-00185 Roma, Italy*

[2]*Istituto Nazionale di Ottica, Consiglio Nazionale delle Ricerche (INO-CNR), Largo Enrico Fermi, 6, I-50125 Firenze, Italy*

[3]*Dipartimento di Fisica and INFN-Sezione di Pavia, via Bassi 6, I-27100 Pavia, Italy*

(Received 23 July 2013; published 26 November 2013)

We demonstrate experimentally the possibility of efficiently detecting properties of quantum channels and quantum gates. The experimentally realized quantum channel detection method has been recently proposed theoretically, and allows us to characterize the properties of quantum channels with a much smaller experimental effort than quantum process tomography. Here, the optimal detection scheme is first achieved for nonentanglement breaking channels of the depolarizing form and is based on the generation and detection of polarized entangled photons. We then demonstrate channel detection for nonseparable maps by considering the CNOT gate and employing two-photon hyperentangled states.

DOI: 10.1103/PhysRevLett.111.220501 PACS numbers: 03.67.Ac, 03.65.Ud, 03.67.Hk, 42.50.Dv

Introduction.—The experimental realization of a quantum channel is unavoidably affected by noise. One possible way to check how well this has been performed is to make a full tomography of the process. This nevertheless is known to be very expensive in terms of the number of measurements to be performed [1]. In many practical situations, however, one is only interested in some specific properties of the experimental channel, e.g., whether it has some entangling power, in order for the channel to be useful for a specific task, such as, e.g., quantum communication.

In this work we address this problem experimentally, following the method of quantum channel detection recently proposed in Refs. [2,3]. The method allows us to detect properties of quantum channels when some *a priori* information about the form of the channel is available. Although being less informative than full process tomography, the method has the advantage of singling out the property of interest with a much smaller experimental effort than in the full tomography case. Moreover, it represents a rough way to bind the noise strength present in the setup; thus, it could serve as a preliminary check in many realistic situations.

The method relies on the concept of witness operators [4] and the Choi-Jamiolkowski isomorphism [5]. We briefly discuss both of them. A state ρ is entangled if and only if there exists a Hermitian operator W such that $\mathrm{Tr}[W\rho] < 0$ and $\mathrm{Tr}[W\rho_{\mathrm{sep}}] \geq 0$ for all separable states; such an operator is called an entanglement witness. The Choi-Jamiolkowski isomorphism gives a one-to-one correspondence between completely positive and trace-preserving maps acting on $\mathcal{D}(\mathcal{H})$ (the set of density operators on $\mathcal{H}$, with finite dimension d) and bipartite density operators $C_{\mathcal{M}}$ on $\mathcal{H} \otimes \mathcal{H}$ (named Choi states). The isomorphism can be stated as $\mathcal{M} \Longleftrightarrow C_{\mathcal{M}} = (\mathcal{M} \otimes \mathcal{I})[|\alpha\rangle\langle\alpha|]$, where $\mathcal{I}$ is the identity map and $|\alpha\rangle$ is the maximally entangled state with respect to the bipartite space $\mathcal{H} \otimes \mathcal{H}$, i.e., $|\alpha\rangle = (1/\sqrt{d}) \sum_{k=1}^{d} |k\rangle|k\rangle$. The above isomorphism can be exploited to link convex sets of quantum channels to particular sets of quantum states. In the following the proposed method will be applied to the convex sets of either entanglement breaking (EB) channels or separable channels.

One-qubit EB channels: Theory.—A channel $\mathcal{M}$ is EB if and only if its Choi state $C_{\mathcal{M}}$ is separable [6]. Therefore, the detection of entanglement of $C_{\mathcal{M}}$ in the doubled system by using a detection operator W_{EB} suitable for $C_{\mathcal{M}}$ allows us to prove that the implemented quantum channel $\mathcal{M}$ is not EB.

We will show the method for the depolarizing channel acting on one qubit, defined as

$$\Gamma_p[\rho] = \sum_{i=0}^{3} p_i \sigma_i \rho \sigma_i, \tag{1}$$

where σ_0 is the identity operator, $\{\sigma_i\}_{i=1,2,3}$ are the three Pauli operators $\sigma_x, \sigma_y, \sigma_z$, respectively, and $p_0 = 1 - p$ (with $p \in [0, 1]$), while $p_i = p/3$ for $i = 1, 2, 3$. Such a channel is known to be EB only for $p \geq 1/2$. Denoting the maximally entangled state of two qubits as $|\Phi^+\rangle$, the corresponding Choi state is given by

$$C_{\Gamma_p} = \left(1 - \frac{4}{3}p\right)|\Phi^+\rangle\langle\Phi^+| + \frac{p}{3}\mathbb{1}, \tag{2}$$

which leads [7,8] to a suitable detection operator of the form [3,7]

$$W_{\mathrm{EB}} = \frac{1}{4}(\mathbb{1} \otimes \mathbb{1} - \sigma_x \otimes \sigma_x + \sigma_y \otimes \sigma_y - \sigma_z \otimes \sigma_z). \tag{3}$$

The detection scheme is depicted in Fig. 1(a). We prepare the two-qubit system in the maximally entangled state $|\Phi^+\rangle$, we then let the depolarizing channel act on qubit 1, and we finally measure the operator W_{EB} acting on both qubits at the end. If $\langle W_{\mathrm{EB}}\rangle < 0$, then we are guaranteed that

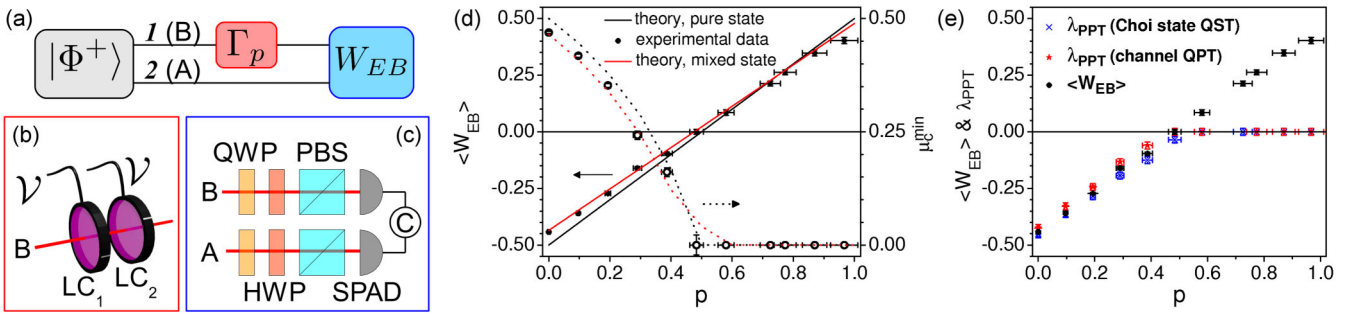

FIG. 1 (color online). (a) Scheme for the one-qubit depolarizing channel detection. $|\Phi^+\rangle$: 2-qubit entangled state; Γ_p: one-qubit depolarizing channel; W_{EB}: EB detection operator measurement. (b) Implementation of the one-qubit depolarizing channel. $\mathrm{LC}_{1,2}$: liquid crystal retarders with axis set at 0° and 45° respectively; $\mathcal{V}$: applied voltage to the LCs. (c) Polarization analysis setup used to evaluate the operator W_{EB}. QWP: quarter-wave plate, HWP: half-wave plate; PBS: polarizing beam splitter; SPAD: single-photon avalanche photodiode; C: coincidence counting electronics. (d) Detection operator value $\langle W_{\mathrm{EB}}\rangle$ (full symbol, solid line) and minimal bound of $\mu_c(\Gamma_p)$ (open symbol, dotted line) as a function of the noise parameter p. (e) Comparison of $\langle W_{\mathrm{EB}}\rangle$ with λ_{PPT} from both the Choi state QST and the channel QPT (see main text).

the depolarizing channel Γ_p is not EB. The theoretical calculated expectation value for the Choi state is $\langle W_{\mathrm{EB}}\rangle = p - 1/2$, which guarantees the detection of all non-EB depolarizing channels, as it gives a negative expectation value whenever $p < 1/2$.

Notice that from the measured $\langle W_{\mathrm{EB}}\rangle$ we can establish a lower bound [3] on the theoretical quantity $\mu_c(\Gamma_p)$ introduced in [9], which represents the minimal amount of noise we need to add to Γ_p via a classical stochastic process in order to make the resulting map EB. Such a bound is given by $\mu_c(\Gamma_p) \geq (2|\langle W_{\mathrm{EB}}\rangle|)/(1 + 2|\langle W_{\mathrm{EB}}\rangle|)$.

One-qubit EB channels: Experiment.—The two-photon states used in this work were produced by a spontaneous parametric down-conversion (SPDC) source operating on the double excitation (back and forth) of a type I beta-barium borate crystal that, depending on the performed experiment, allows us to generate either a polarization entangled state [10] or a path-polarization hyperentangled state [11] of two photons emitted over either two or four spatial modes [see Supplemental Material (SM) for major details [12]].

For this experiment, the two-photon polarization entangled state generated over two spatial modes [Fig. 1(a)] was $|\Phi^+\rangle = (1/\sqrt{2})(|H\rangle_B|H\rangle_A + |V\rangle_B|V\rangle_A)$, where H (V) stands for the horizontal (vertical) polarization of photon A (Alice's) or B (Bob's).

We simulated a one-qubit depolarizing channel, Eq. (1), acting on Bob's photon by inserting two liquid crystal retarders (LC_1 and LC_2) on the path of photon B, one having its fast axis horizontal and the other oriented at 45° with respect to the horizontal [13] [Fig. 1(b)]. Depending on the applied voltage $\mathcal{V}$, it is possible to change the retardation between ordinary and extraordinary polarized radiation. More precisely, by applying either $\mathcal{V}_{\mathbb{1}}$ or $\mathcal{V}_{\pi}$ to a LC, it can be made to act as either a full- or a half-wave plate (HWP), respectively. Thus, by varying independently the voltage applied to LC_1 and LC_2 for different time intervals, we could apply the four Pauli operators to photon B with different values of the weight p (see SM).

To measure the operator W_{EB} given by Eq. (3) as a function of the channel parameter p, we needed to evaluate the expectation values of the three operators $\sigma_x^{\otimes 2}$, $\sigma_y^{\otimes 2}$, and $\sigma_z^{\otimes 2}$ for different values of p that was varied in a controlled way between the extreme values 0 and 1. This was done, for each choice of p, by measuring the coincidences between photons A and B with respect to eight local projectors [14] in the polarization analysis setup which consisted of a quarter-wave plate (QWP), a half-wave plate, a polarizing beam splitter (PBS), and a single-photon avalanche photodiode (SPAD) [Fig. 1(c)]. Note that, if we chose to perform instead either the quantum state tomography (QST) of the two-qubit Choi state or the quantum process tomography (QPT) of the one-qubit channel, at least 16 local projectors would be necessary.

The expectation value of the detection operator is shown in Fig. 1(d), together with the theoretical behavior for a perfectly pure state and the actual one used in the experiment. To compare our results with the theory, we need in fact to take into account the imperfection of the experimentally simulated Choi state. Indeed, the two-photon state produced by the SPDC source corresponds to $|\Phi^+\rangle$ only up to a finite fidelity $F_0 = 0.935 \pm 0.004$ (measured by performing a two-photon quantum state tomography for $p = 0$). Replacing $|\Phi^+\rangle\langle\Phi^+|$ by $F_0|\Phi^+\rangle\langle\Phi^+| + (1 - F_0/3)(|\Phi^-\rangle\langle\Phi^-| + |\Psi^+\rangle\langle\Psi^+| + |\Psi^-\rangle\langle\Psi^-|)$ in Eq. (2), we can thus write the experimental Choi state as $C_{\Gamma_p,\mathrm{expt}} = (1-(4p/3))(4F_0-1/3)|\Phi^+\rangle\langle\Phi^+| + ((p/3)((4F_0-1)/3) + (1-F_0)/3)\mathbb{1}$. The error bars on $\langle W_{\mathrm{EB}}\rangle$ are obtained by propagating the Poissonian uncertainties associated with the coincidence counts, and the error bars on p are estimated by considering the finite response time of the LC.

Let us note that we indeed obtain the EB property of the channel for a value of p up to around 0.5 as expected from

the theory, and as a consequence the bound on $\mu_c(\Gamma_p)$ gets trivial above this value [see Fig. 1(d)]. In Fig. 1(e), we also report for comparison experimental results obtained by performing both the QST of the Choi state and the QPT of the channel. From the QST, we extracted the minimum eigenvalue of the partial transpose of the density matrix [λ_{PPT}(QST)]: we can see that it is indeed negative for $p < 0.5$ and zero for $p \geq 0.5$, as expected, and that it agrees very well with the detection operator $\langle W_{\mathrm{EB}}\rangle$ in the non-EB region. The minimal eigenvalue λ_{PPT}(QPT) was instead calculated from the QPT of the channel: this is also in perfect agreement with $\langle W_{\mathrm{EB}}\rangle$ whenever $p < 0.5$.

Two-qubit separable maps: Theory.—We will now consider the set of separable maps acting on bipartite systems, which are defined as $\mathcal{S}[\rho_{12}] = \sum_k (A_k \otimes B_k)\rho_{12}(A_k \otimes B_k)^\dagger$, where A_k and B_k act on systems 1 and 2, respectively. As for EB channels, the set of separable maps $\mathcal{S}$ is convex, and it is then possible to detect a general map lying outside it. Notice that, since the regarded maps now act on a bipartite state ρ_{12}, the corresponding Choi states refer to a four-partite system 1234 which is separable in the splitting 13–24 [15,16]. As a demonstration of the achievability of the optimal detection method for nonseparable maps, we will consider the explicit case of the CNOT gate. The corresponding detection operator is given by [2,3] $W_{\mathrm{CNOT}} = \frac{1}{2}\mathbb{1} - |\mathrm{CNOT}\rangle\langle\mathrm{CNOT}|$, where $|\mathrm{CNOT}\rangle$ is the Choi state associated with the gate CNOT (with qubit 1 as the target and qubit 2 as the control, and $|\alpha\rangle = |\Phi^+\rangle_{13}|\Psi^+\rangle_{24}$ [17]), namely,

$$|\mathrm{CNOT}\rangle = \frac{1}{\sqrt{2}}(|\Phi^+\rangle_{13}|01\rangle_{24} + |\Psi^+\rangle_{13}|10\rangle_{24}), \qquad (4)$$

where $|\Phi^+\rangle$ and $|\Psi^+\rangle$ are maximally entangled states of the Bell basis. The detection operator above can be measured by using nine different local measurement settings [2,3]. A possible way to reduce the experimental effort is to consider the suboptimal operator [3]

$$\tilde{W}_{\mathrm{CNOT}} = 3\mathbb{1} - 2\left[\frac{(\mathbb{1} + \mathbb{1}\sigma_x^{\otimes 3})}{2}\frac{(\mathbb{1} + \sigma_x\mathbb{1}\sigma_x\mathbb{1})}{2} + \frac{(\mathbb{1} - \mathbb{1}\sigma_z\mathbb{1}\sigma_z)}{2}\frac{(\mathbb{1} + \sigma_z^{\otimes 3}\mathbb{1})}{2}\right], \qquad (5)$$

where we omitted the tensor products and from which it is clear that it requires only two measurement settings.

In this work we also demonstrate the robustness of the detection method when undesired noise is present in the experimental setup. We consider in particular the case of dephasing noise, which is of the form (1) with $p_0 = 1 - q_i$, $p_1 = p_2 = 0$, and $p_3 = q_i$, $i = 1, 2$, and can be implemented in a controlled way in our experiment. We study the case where the dephasing noise acts on both qubits, before and/or after the CNOT gate, as follows [Fig. 2(a)]:

$$\mathcal{M}_{\mathrm{CNOT},\mathcal{D}} = (\mathcal{D}_2 \otimes \mathcal{D}_2)\mathrm{CNOT}(\mathcal{D}_1 \otimes \mathcal{D}_1). \qquad (6)$$

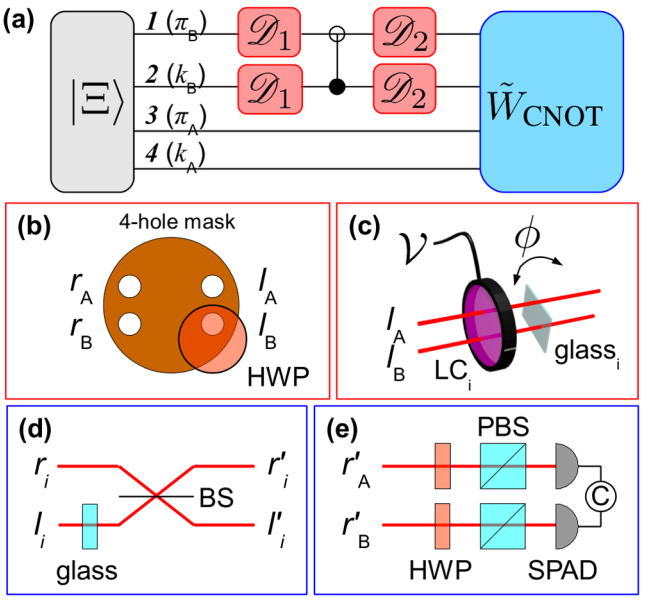

FIG. 2 (color online). (a) Scheme for the two-qubit CNOT channel detection in the presence of dephasing noise. $|\Xi\rangle$: four-qubit hyperentangled state; π_i: polarization qubit; k_i: path qubit, with $i = A, B$; $\mathcal{D}_{1,2}$: independent two-qubit dephasing noise; $\tilde{W}_{\mathrm{CNOT}}$: CNOT detection operator measurement. (b) CNOT implementation. A HWP set at 45° flips the polarization of photon B when its path is l_B. (c) Two-qubit dephasing noise implementation. LC$_i$: liquid crystal retarder with its axis set at 0°; glass i: thin glass plate; $i = 1, 2$. (d) Path analysis setup. Glass: thin glass plate; BS: beam splitter; $i = A, B$. (e) Polarization analysis setup used in combination with (c) to evaluate the operator $\tilde{W}_{\mathrm{CNOT}}$.

Note that the four dephasing processes act independently and are assumed to have the same strength [q_1 (q_2) before (after) the CNOT gate] for the two qubits.

The noise robustness of the operator $\tilde{W}_{\mathrm{CNOT}}$ with respect to dephasing noise is evaluated by the expectation value of $\tilde{W}_{\mathrm{CNOT}}$ given by Eq. (5) with respect to the state $C_{\mathcal{M}_{\mathrm{CNOT},\mathcal{D}}}$ (the Choi state corresponding to the composite map $\mathcal{M}_{\mathrm{CNOT},\mathcal{D}}$), by purposely varying the noise parameters q_1 and q_2 between 0 and 1. We stress that, despite the fact that it requires only two measurement settings, the operator $\tilde{W}_{\mathrm{CNOT}}$ of Eq. (5) turns out to be as efficient as $W_{\mathrm{CNOT}} = \frac{1}{2}\mathbb{1} - |\mathrm{CNOT}\rangle\langle\mathrm{CNOT}|$, in the presence of dephasing noise, since the two operators detect nonseparability of $\mathcal{M}_{\mathrm{CNOT},\mathcal{D}}$ in the same range of values of the noise parameters. Therefore, in the present experiment we measure $\tilde{W}_{\mathrm{CNOT}}$ instead of W_{CNOT}. The theoretical expectation value is given by [3]

$$\mathrm{Tr}[\tilde{W}_{\mathrm{CNOT}} C_{\mathcal{M}_{\mathrm{CNOT},\mathcal{D}}}] = 1 - 2[(1-q_1)^2(1-q_2)^2 + q_1 q_2(1 - q_1 q_2)]. \qquad (7)$$

The roots of the above expression define the threshold values for the noise parameters in order to have a successful nonseparability detection for the noisy map $\mathcal{M}_{\mathrm{CNOT},\mathcal{D}}$.

In case the noise has the same strength before and after the CNOT gate ($q_1 = q_2 = q$), it is possible to detect the nonseparability character of the map for sufficiently low values of the noise parameter: $q < 0.17$. (The case $q_1 \neq q_2$ is further studied in the SM.)

Two-qubit separable maps: Experiment.—For this second experiment, we used the SPDC source operating over four emission modes (see SM). Hence, we prepared the four-qubit hyperentangled state $|\Xi\rangle = |\Phi^+\rangle_{13}|\Psi^+\rangle_{24}$ with $|\Phi^+\rangle_{13} = (1/\sqrt{2})(|H\rangle_B|H\rangle_A + |V\rangle_B|V\rangle_A)$ and $|\Psi^+\rangle_{24} = (1/\sqrt{2})(|r\rangle_B|l\rangle_A + |l\rangle_B|r\rangle_A)$, where r (l) stands for the right (left) path of photon A or B.

We implemented a CNOT gate on Bob's photon by inserting a half-wave plate set at 45° on the left path of photon B; thus, the path (qubit 2) acts as the control and the polarization (qubit 1) acts as the target [Fig. 2(b)]. After the CNOT gate, the four-qubit state then reads as $|\Xi_{\text{out}}\rangle_{1234} = \frac{1}{2}(|Hr\rangle_B|Hl\rangle_A + |Vl\rangle_B|Hr\rangle_A + |Vr\rangle_B|Vl\rangle_A + |Hl\rangle_B|Vr\rangle_A)$. Using the correspondence $|H\rangle_{B,A} \leftrightarrow |0\rangle_{13}$, $|V\rangle_{B,A} \leftrightarrow |1\rangle_{13}$, $|r\rangle_{B,A} \leftrightarrow |0\rangle_{24}$, and $|l\rangle_{B,A} \leftrightarrow |1\rangle_{24}$, this is equivalent to the Choi state of the CNOT channel expressed in the logical basis (4).

Dephasing noise was simulated by acting independently on qubits 1 and 2, before and/or after the CNOT gate, as in Eq. (6), by inserting a LC with its fast axis at 0° with respect to the horizontal and a thin glass plate, both before and after the CNOT [Fig. 2(c)]. Each LC induces a phase between $|H\rangle_B$ and $|V\rangle_B$ that can be set to either 0 or π by applying a voltage $\mathcal{V}_{\mathbb{1}}$ or $\mathcal{V}_{\pi}$, respectively, thus acting either as $\mathbb{1}$ or σ_z for qubit 1; each glass plate introduces a phase ϕ between $|r\rangle_B$ and $|l\rangle_B$ that can be set to 0 or π by calibrated rotations of the plate, thus acting either as $\mathbb{1}$ or σ_z for qubit 2. By varying the relative time of action of each dephaser, in a similar manner as in the one-qubit channel experiment, we were able to vary the values of q_1 and q_2.

To measure the detection operator $\tilde{W}_{\text{CNOT}}$ (5) as a function of q_1 and q_2, we needed to evaluate the expectation values of the two operators $\sigma_x^{\otimes 4}$ and $\sigma_z^{\otimes 4}$ for several values of q_1 and q_2. Thus, for each value of q_1 and q_2, we measured coincidence counts between photons A and B by using 32 local projectors in the polarization-path analysis setup. The polarization analysis in this case is achieved via a HWP and a PBS [Fig. 2(e)] while the path analysis is done either by directly sending the photons to the detectors (thus measuring $|r\rangle$ and $|l\rangle$) or by passing them first through a beam splitter and a thin glass plate [thus measuring $|d\rangle = (1/\sqrt{2})(|r\rangle + |l\rangle)$ and $|a\rangle = (1/\sqrt{2})(|r\rangle - |l\rangle)$] [Fig. 2(d)]. Note that, in this case, the QST on the Choi state or the QPT on the channel would require at least 256 local projectors instead of 32. In general, the number of measurement settings required by the QST on the Choi state or the QPT scales as d^4 (d being the dimension of the Hilbert space on which the channel acts), while for the proposed experimental method it scales at most as d^2 [3,18].

We obtained the detection operator values reported in Fig. 3 as a function of $q_1 = q_2 = q$. Again, to compare

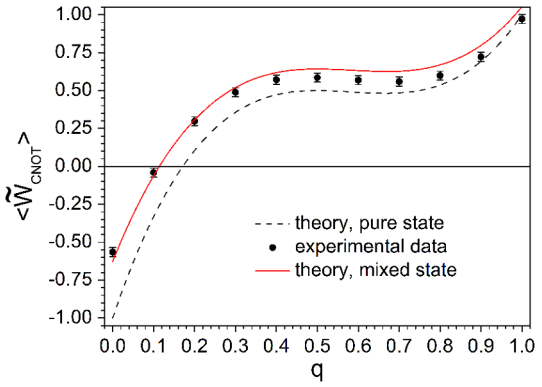

FIG. 3 (color online). CNOT detection operator value $\langle \tilde{W}_{\text{CNOT}} \rangle$ as a function of the noise parameter q.

them properly with the theory, we must take into account the finite purity of the initial Choi state that we prepared to simulate the Choi state of the CNOT gate. We could model the experimental Choi state of the CNOT noisy channel, given the visibilities (measured in the diagonal basis) of the polarization ($\nu_\pi = 0.858 \pm 0.008$) and path ($\nu_k = 0.904 \pm 0.004$) entanglement for $q = 0$ (see SM). As can be seen, our results are in good agreement with the theoretical calculation. Note that the slight discrepancy remaining for large q is probably due to imperfections in the simulated dephasing noise. As expected, from these results it is evident that even a low level of noise makes the CNOT to no longer be an entangling gate; in particular, the nonseparability of the map is no longer detected for $q > 0.1$ in our experiment.

Conclusion.—We have implemented a method that allows us to check the entanglement properties of a noisy multiqubit gate with fewer measurements than those required by a full quantum process tomography and could thus be a more convenient tool for routine performance checks on quantum gates. Moreover, the experimentally implemented method provides upper bounds on the noise strength and thus could be useful to test whether the quantum channel under consideration is noiseless enough to guarantee the realization of a given quantum information task. This method has been tested in the cases of a one-qubit entanglement breaking channel and of a two-qubit separable map with very good agreement between experimental measurements and theoretical predictions. Finally, we would like to stress that the reported techniques can be, in principle, adapted to test EB or separability properties of any quantum gates or channels, and in the presence of any noise process affecting the experimental situation considered. The present experimental demonstration therefore opens the way to a wide range of applications of the detection techniques to other gates or channels and different noise processes that can be of interest in many other physical scenarios, ranging from atomic to solid-state physics.

The work was supported by the EU Project QWAD (Quantum Waveguides Applications & Developments).

*adeline.orieux@gmail.com; http://quantumoptics.phys.uniroma1.it/

[1] See, for example, M. A. Nielsen and I. L. Chuang, *Quantum Computation and Quantum Information* (Cambridge University Press, Cambridge, England, 2000).

[2] C. Macchiavello and M. Rossi, Phys. Scr. **T153**, 014044 (2013).

[3] C. Macchiavello and M. Rossi, Phys. Rev. A **88**, 042335 (2013).

[4] M. Horodecki, P. Horodecki, and R. Horodecki,Phys. Lett. A **223**, 1 (1996); B. M. Terhal,Phys. Lett. A **271**, 319 (2000).

[5] A. Jamiolkowski, Rep. Math. Phys. **3**, 275 (1972); M.-D. Choi, Linear Algebra Appl. **10**, 285 (1975).

[6] M. Horodecki, P. W. Shor, and M. B. Ruskai, Rev. Math. Phys. **15**, 629 (2003).

[7] O. Gühne, P. Hyllus, D. Bruß, A. Ekert, M. Lewenstein, C. Macchiavello, and A. Sanpera, Phys. Rev. A **66**, 062305 (2002).

[8] O. Gühne, P. Hyllus, D. Bruß, A. Ekert, M. Lewenstein, C. Macchiavello, and A. Sanpera, J. Mod. Opt. **50**, 1079 (2003).

[9] A. De Pasquale and V. Giovannetti, Phys. Rev. A **86**, 052302 (2012).

[10] C. Cinelli, G. Di Nepi, F. De Martini, M. Barbieri, and P. Mataloni, Phys. Rev. A **70**, 022321 (2004).

[11] M. Barbieri, C. Cinelli, P. Mataloni, and F. De Martini, Phys. Rev. A **72**, 052110 (2005).

[12] See Supplemental Material at http://link.aps.org/supplemental/10.1103/PhysRevLett.111.220501 for major details on the experimental setups and the CNOT channel results.

[13] A. Chiuri, V. Rosati, G. Vallone, S. Pádua, H. Imai, S. Giacomini, C. Macchiavello, and P. Mataloni, Phys. Rev. Lett. **107**, 253602 (2011).

[14] M. Barbieri, F. De Martini, G. Di Nepi, P. Mataloni, G. M. D'Ariano, and C. Macchiavello, Phys. Rev. Lett. **91**, 227901 (2003).

[15] E. M. Rains, arXiv:quant-ph/9707002.

[16] J. I. Cirac, W. Dür, B. Kraus, and M. Lewenstein, Phys. Rev. Lett. **86**, 544 (2001).

[17] Here we implement the Choi state corresponding to the gate CNOT by starting from the maximally entangled state $|\Phi^+\rangle_{13}|\Psi^+\rangle_{24}$ instead of $|\Phi^+\rangle_{13}|\Phi^+\rangle_{24}$. This choice, besides not affecting the techniques, will be more convenient in the experimental realization that follows.

[18] A. G. White, A. Girlchrist, G. J. Pryde, J. L. O'Brien, M. J. Bremner, and N. K. Langford, J. Opt. Soc. Am. B **24**, 172 (2007).